

# Scribbles to Vectors: Preparation of Scribble Drawings for CAD Interpretation

A. Bartolo, K. P. Camilleri, S. G. Fabri, J. C. Borg and P. J. Farrugia

Faculty of Engineering, University of Malta, Malta

---

## Abstract

*This paper describes the work carried out on off-line paper based scribbles such that they can be incorporated into a sketch-based interface without forcing designers to change their natural drawing habits. In this work, the scribbled drawings are converted into a vectorial format which can be recognized by a CAD system. This is achieved by using pattern analysis techniques, namely the Gabor filter to simplify the scribbled drawing. Vector line are then extracted from the resulting drawing by means of Kalman filtering.*

Categories and Subject Descriptors (according to ACM CCS): I.4.3 [Image Processing and Computer Vision]: Filtering I.4.7 [Image Processing and Computer Vision]: Texture

---

©ACM, (2007). This is the author's version of the work. It is posted here by permission of ACM for your personal use. Not for redistribution. The definitive version was published in the proceedings of the Eurographics Workshop on Sketch-Based Interfaces and Modelling, 2007

## 1. Introduction

Unconstrained sketching in early design is important. This fact is evident by the number of researchers that strive to create sketch-based interfaces that give the user the maximum freedom possible, aiming at obtaining a transparent, easy to use interface. The trend in these interfaces is to give the designer the impression that the drawing is made using traditional pen and paper, possibly through the use of digital pens and Tablet PCs. However, the freedom and flexibility available to designers when using traditional pen and paper remains unparalleled and this is evident in the lower adoption rates of Tablet PCs [NM04]. Using pen-and-paper, designers may benefit from quick, uninterrupted sketching, allowing the designer to focus on the design of the object rather than the interactions required with the interface system. This in turn makes the designers more likely to explore different design solutions, hence increasing the creativity of their designs [SL97].

This flexibility has a price. Paper is a passive medium and through paper alone, the designer cannot obtain the 3D ren-

dered models that may be obtained through CAD systems. To obtain such models, the designer must redraw the sketch, either using the CAD tool directly, or by using an intermediary sketch based interface. Hence the need of an interpretation technique that may integrate the paper-based drawing with CAD systems. In our previous work [FBCG06], [BCFB06], we have demonstrated a possible solution, using a prescribed sketching language to facilitate the interpretation of paper-based drawings. This work further improves our previous interface by allowing the designer to sketch the object profile using multiple strokes or scribbles; thereby increasing the designer's drawing freedom. This paper focuses on the simplification of the scribbled profile such that the scribble may be represented by vector data which may be imported into a CAD system. The designer is limited to drawing the profile of the object since this paper does not tackle the issues involved in shading strokes.

The rest of the paper is organized as follows: Section 2 gives a brief review of the methods used to interpret scribbled drawings, Section 3 describes the use of Gabor filtering techniques for perceptual simplification, Section 4 describes how the Kalman filter framework may be used to extract a vectorial representation of the simplified scribble whilst Section 5 concludes the paper with a discussion on the work.

## 2. Background

Given drawing freedom, designers would draw initial sketches using over-traced scribbles. Interpretation of these scribbles requires the grouping of the over-traced line strokes into a single line vector. Vectorization of neat sketches and technical drawings is a well researched area, with robust algorithms such as SPV [LD99] and OOPSV [SSC\*02] being well established in literature. These techniques however consider each line stroke in the image as an intended distinct line, such that should these algorithms be applied to scribbled drawings, the vectorization technique would attempt to represent all over-traced line strokes as separate vectors. Since the over-traced strokes intersect each other, such techniques would be required to treat as junction points a number of ‘false junctions’, that is, intersections of the scribbled over-strokes which are not intended to be perceived as junctions. These ‘false junctions’ are problematic in that they increase the computational complexity of the algorithms considerably. For example, in graph-based techniques such as [HT06], junctions are represented as graph nodes hence increasing the size of the graph structure representing the drawing.

The problem of selecting an intended shape amongst a clutter of line fragments has been tackled through perceptual grouping techniques rather than through vectorization. In these methods, the Gestalt laws are applied in order to select paths that are more salient than others. Thus authors such as Saund [Sau03] and Estrada and Jepson [EJ04] search for long paths that form convex closed contours, giving preference to smooth paths that form object profiles rather than to meandering paths. However, these techniques have a major flaw, namely, the assumption that the clutter of line segments is due to some unrelated background rather than to supporting line strokes. In fact, using the criteria described in [Sau03] and [EJ04] to identify preferred paths results in a number of equally salient line paths.

Simplification of paper-based scribbles has, as yet, been unchallenged. However, scribbled drawings are being tackled by on-line based systems such as those described in [KS06] and [KQW06]. In these systems, the interpretation process has access to the sequence with which the strokes are drawn. Thus simplification of the scribbled drawing is carried out in real-time by comparing each new stroke to a bank of existing strokes. Such a simplification cannot however be applied to paper-based sketches since the sequence of line strokes is unknown. Furthermore, in on-line systems, each line stroke is extracted as a whole entity irrespective of the number of line strokes that are intersected when drawing the stroke. The same cannot be applied to off-line paper-based drawings where the vectorization process would split the line strokes into smaller fragments at line junctions.

An alternative simplification procedure is that described in [SD04]. This uses a point cloud thinning approach to cluster foreground pixel locations to some best fitting line. The

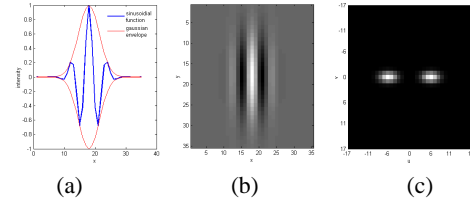


**Figure 1:** Gabor Filter with  $\sigma = 3.37$ ,  $\theta = 0$ ,  $\lambda = 6$ ,  $\gamma = 0.5$  and  $\phi = 0$ . (a) Scan along the x-axis showing the sinusoidal function superimposed upon the Gaussian envelope, (b) the Gabor filter in the space domain, (c) the power spectrum of the filter.

disadvantage of this technique, as with other thinning-based vectorization methods is the poor performance at the junction regions. At junctions, the foreground pixels from different line directions cause the medial axis to deviate from the true intersection point of the two lines.

In view of the difficulties that exist in the simplification of paper-based scribbles, Saund [Sau03] suggests that the perceptual grouping techniques used to identify salient paths should be applied after a pre-processing step that makes use of pattern recognition techniques. Following on this suggestion, the use of the co-occurrence matrix was suggested in [BCFB06]. The co-occurrence matrix may be used to group line strokes that fall within a tolerance region. The drawback of this method is that the minimum tolerance region must be large enough to obtain a well-define co-occurrence matrix, placing a lower bound on the minimum distance between pairs of parallel line groups hence limiting the resolution of the drawing.

## 3. Gabor Filtering for Scribble Simplification

The Gabor filter, governed by Equation 1 and whose impulse response is given in Figure 1 is parameterized by the the spatial frequency  $\frac{1}{\lambda}$  and phase  $\phi$  of the sinusoidal function, as well as the spatial width  $\sigma$ , aspect ratio  $\gamma$  and orientation  $\theta$  of the Gaussian function [GPK02].

$$g_{\sigma,\theta,\lambda,\gamma,\phi}(x,y) = \exp\left\{-\frac{1}{2\sigma^2}(\hat{x}^2 + \gamma^2\hat{y}^2)\right\} \cos\left(\frac{2\pi}{\lambda}\hat{x} + \phi\right) \quad (1)$$

$$\hat{x} = x \cos \theta + y \sin \theta$$

$$\hat{y} = y \cos \theta - x \sin \theta$$

The filter may be compared to the response given by the cells in the human visual cortex in that the filter is frequency and orientation selective and responds to single bars as well as gratings, imitating the simple and complex cells of the human visual cortex [Hub95]. Frequency and orientation selectivity is obtained by varying the spatial frequency  $\frac{1}{\lambda}$  and the orientation  $\theta$  of the sinusoidal function for a given spatial spread  $\sigma$ . In order to further imitate the human visual

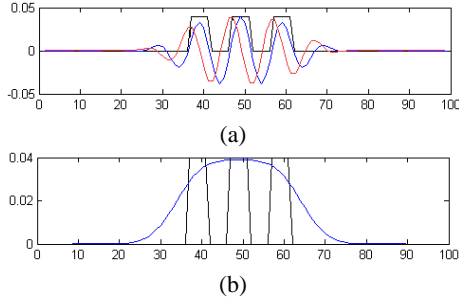


**Figure 2:** Response of a Gabor filter with wavelength  $\lambda = 10$  for a sequence of three bars. A phase of  $\phi = 0$  radians (blue plot in (a)) responds to the bar centres, a phase of  $\phi = \frac{\pi}{2}$  radians (red plot in (a)) gives better response at the bar edges while the Gabor energy (b) combines the two responses giving a continuous response over all over-traced regions.

system, this spatial spread is often related to the spatial frequency, using the ratio  $\frac{\sigma}{\lambda}$  equal to 0.56 [GPK02]. This results in a filter bandwidth of one octave which is thought to be the bandwidth of the human receptive field.

By changing the phase of the sinusoidal function, one may vary the area of the scribble stroke to which the filter responds. As shown in Figure 2, with phase shift of  $\phi = 0$  rad, the filter responds mostly to the centre of the bars, whereas with a phase shift of  $\phi = \frac{\pi}{2}$  rad, the filter responds to the bar edges. Since the Gabor filter is being used to group over-traced scribbles into single line groups, the filter should give a maximum continuous response for the bars, the intra-line gaps between the bars and the bar edges. This is obtained by combining the Gabor filters having a phase of  $\phi = 0$  rad and  $\phi = \frac{\pi}{2}$  rad creating a quadrature filter which may be described in terms of the Gabor energy given by Equation 2

$$G_{\sigma,\theta,\lambda,\gamma} = \sqrt{g_{\sigma,\theta,\lambda,\gamma,\phi=0}^2 + g_{\sigma,\theta,\lambda,\gamma,\phi=\frac{\pi}{2}}^2} \quad (2)$$

### 3.1. Selection of a filter bank

Since the designer drawing the scribble is not concerned with the creation of patterns, the drawing is not expected to have a consistent grating pattern throughout the edge profile. The width of a perceived over-traced stroke group depends on the thickness of the pen, the resolution with which the drawing is digitized as well as the density of the over-strokes. The combination of these three factors determines the frequency to which the filter would respond mostly. Although pen thickness and resolution remain constant for a given image, the density of the over-strokes varies such that a filter bank is required in order to obtain a constant response for all over-traced regions. The filter bank must be selected such that it gives a good coverage of the frequency spectrum. Given any pen thickness and resolution, a minimum wavelength of two pixels is necessary in order to resolve two line strokes. This acts as a lower bound to the frequency

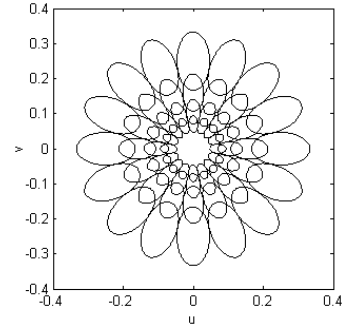


**Figure 3:** The Spatial-frequency domain coverage corresponding to a 32 filter bank.

range of the filter. The largest wavelength possible however depends on the pen thickness and resolution of the image, both of which can vary for different images. Assuming that the largest wavelength is ten times larger than the smallest permissible wavelength, the required frequency range would then be of  $[2 \cdots 20]$  pixels. Since the Gabor filter acts as a band-pass filter and a frequency bandwidth of one octave is being assumed, a four level filter bank with centre wavelengths of  $[4, 6.25, 9.43, 14.28]$  pixels is required to provide coverage for the selected frequency range.

It is also necessary to select a range of orientations such that the filter may respond equally well to all line orientations. Given the frequency bandwidth selected, the angular resolution of the Gabor filter is of  $0.105\pi$  rad. However, given the nature of the scribble, orientations that are integer multiples of  $\frac{\pi}{4}$  are more common than other line orientations. Thus, the angular resolution was slightly decreased to  $\frac{\pi}{8}$  allowing the filter bank to tune to these preferred orientations. This results in eight filters for each level of the filter bank, hence a total of 32 filters as shown in Figure 3.

The individual filters in the filter bank give an indication of the preferred frequency and orientation of regions in the scribble. From these 32 individual responses, eight orientation response images may be obtained by grouping the responses at each frequency level  $j \in [1 \cdots 4]$  for each orientation  $\theta_i, i \in [1 \cdots 8]$ . These orientation response images can therefore be defined as  $R_i = \max_{\lambda} \{G_{\sigma,\theta_i,\lambda,\gamma}\}$  and may be used as an indication of the degree of matching between a pixel's neighbourhood and the selected filter orientation. Thus, the orientation of the scribbled line strokes passing through a particular pixel location may be determined by evaluating the maximum value of  $R_i$  at that location. The eight orientation response images may be further grouped into a single response image  $Q$  such that  $Q = \max_i \{R_i\}$ . This single response image gives an indication of the line strokes that may be grouped into a single line group, hence simplifying the image. However, as shown in Figure 4, although the quadrature Gabor filter bank allows the grouping of the over-traced line strokes, and the response is lower at the inter-line gaps, the quadrature filter bank alone can-

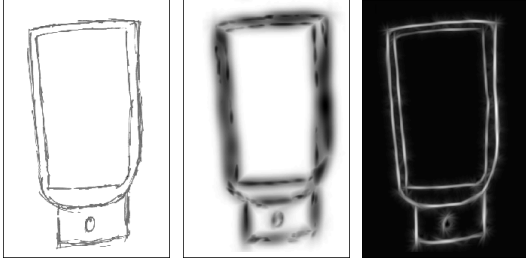


**Figure 4:** The result obtained after applying the filter banks to the a scribble shown in (a). The overall response of the quadrature filter  $Q$  is given in (b) while the response of the 'centre off' filter is given in (c). Note that in (b) and (c) dark regions indicate regions where the filter response is high.

not provide sufficient discrimination between distinct line groups in the drawing.

### 3.2. Detecting the inter-line gaps

Distinction between different line groups may be obtained if there is sufficient contrast between the two line groups such that an inter-line gap is detected. In general, distinction between over-traced line groups can be made if the inter-line gap is greater than the width of the intra-line gaps present within the line group. This indicates that inter-line gaps may be detected by Gabor filters that have a coarser spatial frequency than that used by the quadrature filter to group the over-traced strokes. At this coarser frequency bandwidth, line groups separated by an inter-line gap may be considered as forming an on-off-on grating and the Gabor filter is required to detect this patten. This implies that the inter-line gaps may be detected by using 'centre-off' filters having a half response spatial frequency bandwidth of two octaves, hence setting the ratio  $\frac{\sigma}{\lambda} = 0.3123$  and phase  $\phi = \pi$  rad. As shown in Figure 4 using this filter, inter-line gaps give a positive response whereas the line stroke group give a negative response, hence distinction between the line group and the inter-line gap can be carried out using a 'centre-off' filter without requiring the use of a quadrature filter.

In this application, it is assumed that the width of the inter-line gap is greater than the width of the line strokes such that the filter bank is required to cover a range of wavelengths starting from 14 pixels. Theoretically, there is no limit on the maximum inter-line gap since a single line group may be considered as having an infinite inter-line gap. However, for practical reasons, the filter bank was limited to a maximum wavelength that is ten times greater than the smallest inter-line gap. Thus, the range of wavelengths is required to be  $\lambda = [14 \cdot \dots \cdot 140]$  pixels. Given the larger frequency bandwidth this frequency range may be obtained using two frequency levels, corresponding to  $\lambda = 22$  and  $\lambda = 66$ . The larger frequency bandwidth also reduces the orientation resolution to  $\frac{\pi}{6}$  such that as shown in Figure 5 a 12-filter bank is sufficient to detect the inter-line gaps.

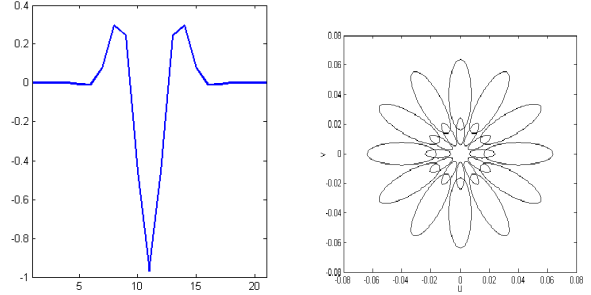


**Figure 5:** The Gabor filter that detects inter-line gaps. (a) The filter profile (b) the spatial-frequency domain coverage of the filter bank. (Note the scale difference with respect to Figure 3)

The responses obtained for this filter bank are grouped into a single response  $I$  defined as  $I = \max_{\theta} \max_{\lambda} \{G_{\sigma, \theta, \lambda, \gamma}\}$ . This response is used to inhibit the inter-line gaps in the quadrature filter response  $Q$  such that a final response image that groups line strokes while distinguishing between different line groups may be defined by Equation 3.

$$Q(x, y) = \begin{cases} Q(x, y) & \text{if } I(x, y) < 0 \\ 0 & \text{if } I(x, y) \geq 0 \end{cases} \quad (3)$$

### 4. Vectorization of the Scribbled Drawing

The result obtained after processing the scribbled drawing using the Gabor filter is similar to the neat sketches processed by traditional vectorization techniques such that line vectors may be obtained from a binary representation of the Gabor filter response image  $Q$ . However, such techniques would ignore the orientation information obtained by the Gabor filter, only to recompute or approximate the line orientations. Furthermore, the vectorization techniques described in literature do not take into account the noise present in the image. Thus, although the image noise affects the position of the medial axis, it is not considered in the evaluation of the medial axis. Rather than using standard vectorization techniques, this work extends further the concept of line tracking using the Kalman filter described in our previous work [BCF\*05], in order to obtain the required line vectors.

The scribbled line stroke may be modeled by a pen moving along a trajectory in a piecewise linear manner such that the position of the pen defined by its  $(x, y)$  co-ordinates at any instant  $k$  may be written as

$$\begin{aligned} x_{k+1} &= x_k + \Delta x_k \\ y_{k+1} &= y_k + \Delta y_k \end{aligned} \quad (4)$$

where  $\Delta x_k$  and  $\Delta y_k$  reflect the gradient of the trajectory at an instant  $k$  and are determined from the orientation response of the Gabor filter. However, the orientation estimate may have an error of up to  $\frac{\pi}{16}$  due to the orientation resolution

of the Gabor filter such that better measurements of the pen position are required. This may be obtained by taking a scan line perpendicular to the curve at the point  $(x_{k+1}, y_{k+1})$  such that the medial point of the line may be evaluated. In this way, the scribble may be considered as a process modeled by Equation 4 having a state vector  $\mathbf{X} = [x, y]^T$  and input  $\mathbf{U} = [\Delta x, \Delta y]^T$ . From the original image, measurements giving the position of the medial points may be obtained. By considering these measurements as the output of noisy sensors, the Kalman filter may be used to estimate the system states, hence obtain better estimates of the medial axis.

The Kalman filter assumes that a system is governed by a discrete time process modeled by the linear stochastic equation given by Equation 5 for which a measurement  $\mathbf{Z}$  may be related to its state  $\mathbf{X}$  using Equation 6 [May79].

$$\mathbf{X}_k = A\mathbf{X}_{k-1} + B\mathbf{U} + \mathbf{W}_{k-1} \quad (5)$$

$$\mathbf{Z}_k = H\mathbf{X}_k + \mathbf{V}_k \quad (6)$$

where  $\mathbf{W}$  and  $\mathbf{V}$  are random variables representing the process and measurement noise respectively which are assumed to be white gaussian noise processes having zero mean and co-variance of  $Q$  and  $R$  respectively. Comparison between Equations 4 and 5 indicates that  $A$  and  $B$  are identity matrices of size  $2 \times 2$ . Furthermore, the measurements of the medial axis points are directly related to the system states such that the function  $H$  in Equation 6 can also be represented by a  $2 \times 2$  identity matrix. In this application, the process noise models the deviations of the true trajectory from the estimated trajectory obtained through the process model. This deviation is due to the resolution error of the Gabor filter orientation estimate. In the worst case, an error of  $\frac{\pi}{16}$  rad is obtained and this error is used to model the process noise covariance. The measurement noise represents the error in the measurements of the medial axis points. This is due to the changes in line width which displace the medial axis point from its true location. Thus an estimate of the measurement noise is obtained by observing the changes in line width along the trajectory.

The Kalman filter performs the state estimation in two steps, denoted as the time update and measurement update steps such that feedback obtained from the measurements  $\mathbf{Z}$  are used to obtain better estimates of the states  $\mathbf{X}$ . In the time update step given by Equations 7 the a priori state estimate  $\mathbf{X}_{k|k}$  and the error covariance,  $P_{k|k}$  is obtained using the process model and the a posteriori state  $\mathbf{X}_{k|k-1}$  and error covariance  $P_{k|k-1}$ . These are then updated in the measurement update step give by Equations 8, using the actual measurement  $M_k$  and the gain matrix  $K$  which minimizes the a posteriori error covariance

$$\begin{aligned} X_{k|k-1} &= AX_{k-1|k-1} + BU_{k-1|k-1} \\ P_{k|k-1} &= AP_{k-1|k-1}A^T + Q \end{aligned} \quad (7)$$

$$\begin{aligned} K_k &= P_{k|k-1}H^T(HP_{k|k-1}H^T + R)^{-1} \\ X_{k|k} &= X_{k|k-1} + K_k(M_k - HX_{k|k-1}) \\ P_{k|k} &= (I - K_kH)P_{k|k-1} \end{aligned} \quad (8)$$

## 5. Evaluation

The result shown in Figure 10 illustrates that the Gabor filter simplifies the scribble sufficiently such that vectorization of the scribbled drawing may be carried out without resulting in a large number of vector data. The goodness of fit of the vector representation depends on two factors, namely the accuracy with which the orientation is estimated as well as the fidelity with which the Gabor response represents the designer's intent. The estimation of the Gabor orientation is known to have an error of  $\frac{\pi}{16}$  rad and this is in fact included in the Kalman Filter process noise model. However, it is essential that within this resolution, the error in orientation estimates remains consistent for any image conditions, including noisy digitizations. In order to test this, a ground truth image consisting of a single line bar was rotated at intervals of  $10^\circ$ . Increasing the image noise causes the Gabor energy to decrease reaching a decrease of up to 50% for a noise level of  $-30$ dB SNR, indicating a decrease in the certainty of the orientation estimate. However, although the certainty in the estimate has decreased, the orientation estimates remain consistent and no increase in error is observed. This contrasts with the orientation estimates obtained by Sobel edge detection which is sometimes used in vectorization and perceptual grouping algorithms where an mean error increase of  $6^\circ$  was observed.

The fidelity of the Gabor filter response to the designer's intent was also compared with the results obtained by an off-the-shelf binarization technique. As shown in Figure 6 the number of misclassified pixels obtained by the Gabor response is initially higher due to a thickening of the lines on all sides of the line and therefore this error does not affect the vectorization stage. One may note that the number of misclassified pixels remains constant for up to a noise level of  $-30$ dB SNR in contrast to the increase of  $80$ dB in the number of misclassified pixels at an SNR level of  $-20$ dB obtained by the binarization algorithm.

As has been discussed earlier, the response of the Gabor filter is dependant on the resolution with which the image is digitized since this changes the number of pixels with which the lines are represented, hence the wavelength of the scribbled strokes. In order to evaluate the effect of different resolutions for the particular Gabor filter bank indicated, the response of the Gabor filter to test scribbles such as that shown in Figure 7 was observed under different image resolutions. Using this test image, the response of the Gabor filter was also compared to the results that are obtained when using standard morphology techniques, namely the *close* operation with a circular structural element having a radius

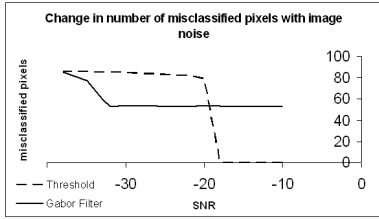


**Figure 6:** The change in number of misclassified pixels with increasing noise levels. Note that the number of misclassified is given in dB

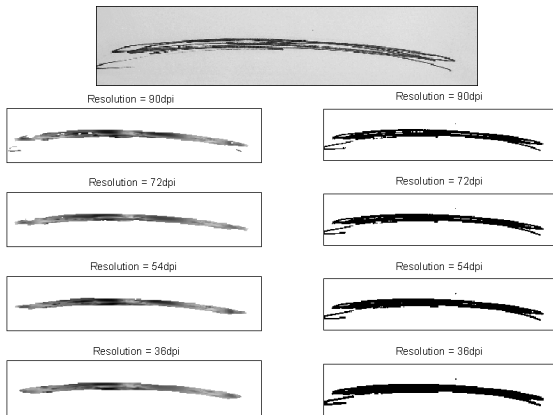


**Figure 7:** Illustrating the performance of the filter bank for the test scribble shown above under different resolutions and comparison of the results with those obtained after applying the close operation with a circular structural element of radius 5 pixels

of 5 pixels. The number of true positives (TP), false positives (FP) and false negative (FN) matches were recorded for a resolution range between 36dpi and 92dpi. The Gabor filter obtained mean values of  $TP = 87\%$ ,  $FP = 13\%$ ,  $TP = 0.75\%$  whereas the *close* operation obtained mean values of  $TP = 89\%$ ,  $FP = 11\%$ ,  $TP = 2.83\%$ . The increase of the line boundaries described previously causes the Gabor filter to obtain a larger number of false positives than the *close* operation, however, the Gabor filter obtains lower false negative scores, indicating that, as shown in Figure 7, the Gabor filter is more suitable than the morphology operator in grouping over-traced line strokes. These results also show that the filter bank selected gives accurate responses for a range of resolutions of up to 56dpi. An increase or decrease in the image resolution beyond this range requires an equivalent shift in the center frequencies of the filter bank.

Figure 8 further illustrates the role of the ‘centre-off’ filter bank. These plots show the filter response for two groups of parallel gratings having a total width of 20 pixels. The

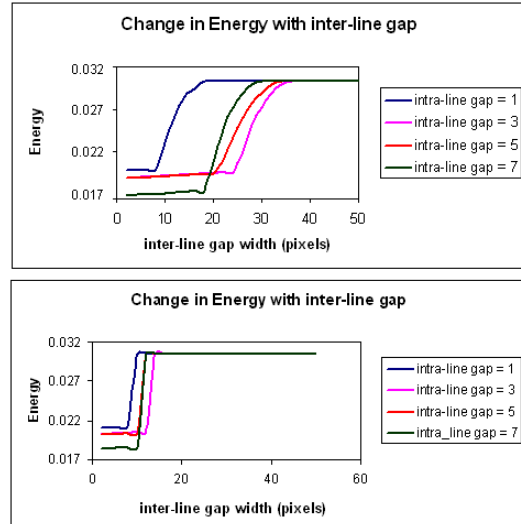


**Figure 8:** Comparison of the quadrature filter response and the inhibited quadrature filter response, illustrating the effect of the ‘centre-off’ filter.

intra-line gap of the test pattern was varied creating different grating patterns and the Gabor energy at the centre of the inter-line gap between the grating groups was recorded for the quadrature filter alone as well as for the inhibited quadrature filter. For the purpose of this test, a single level ‘centre-off’ filter bank having a centre frequency of 0.025 pixels was used. Using such a filter, the minimum gap width to which the filter responds is of 12 pixels. Thus, as shown in Figure 8, distinction between two line groups can be made for inter-line gaps that are smaller than the global width of the line group. Correct classification of over-strokes can be obtained providing that the intra-line gap is smaller than the minimum frequency selected. Thus, depending on the roughness with which the scribble is drawn, the ‘centre-off’ filter bank may be shifted in the frequency domain such that stroke groups are split only at inter-line gaps and not at intra-line gaps. This also implies that the Gabor filter is mostly useful for scribbles drawn with approximately the same level of roughness. Scribbles such as that shown in Figure 9 are not grouped into a single line group since at a signal level, these over-strokes cannot be distinguished from other over-stroke groups that belong to a different line group. Such scribbles require post-processing that uses the semantic information available through a global perception of the scribble region. However, in such cases, using the Gabor filter to group over-traced strokes for which the intra-line gap is sufficiently smaller than the inter-line gap simplifies the scribble and hence any other necessary post-processing.

The performance of the Kalman filter vectorization algorithm was compared to the SPV algorithm which is well established in literature, using the suggested pixel recovery

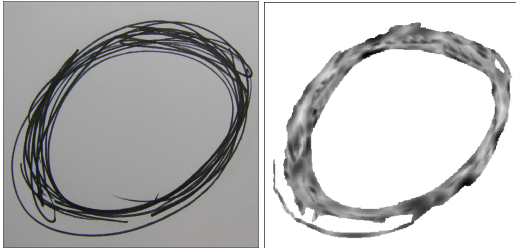


**Figure 9:** Over-traced line strokes can be grouped together providing that the intra-line gap is smaller than the inter-line gap. Thus, over-strokes with wide intra-line gaps which are perceived as single line groups require further post-processing that incorporates global semantic information about the image.

index (PRI) in order to compare performance [LD99]. In order to provide a fair comparison, the SPV algorithm was performed on a binarized version of the Gabor filter, rather than the scribble drawing itself. For the scribbles tested, the Kalman filter obtained a mean PRI of 0.84, whereas the SPV algorithm obtained a PRI of 0.82. Thus the performance of the Kalman filter is comparable to that of the SPV. The computational time for the Kalman filter and the SPV algorithm are similar, however, the Kalman filter returns a smaller number of vectors, thus performing the tracking in a shorter time period.

## 6. Conclusions

This work has presented a novel scribble simplification procedure whereby the Gabor filter is used to group over-traced line strokes into their respective line groups which are subsequently represented as line vectors by tracking the edge-profile using the Kalman filter. Grouping of over-strokes is carried out using two filter banks, such that over-traced regions are identified using a quadrature filter bank while inter-line gaps separating the line groups are identified through a centre-off filter bank. The response of this second filter bank is used to inhibit quadrature filter response at the inter-line regions, hence allowing the separability of distinct line groups. Although the Gabor filter bank is defined for eight discrete orientations, the Kalman filter trajectories are not constrained to follow these discrete orientations. Over-traced line strokes whose orientation is equidistant from the orientation of a pair of quadrature filters will cause both filters to respond equally strongly. Since the Kalman filter uses the eight oriented measurements  $R_1 \dots R_8$  obtained from the quadrature filter bank to update the filter states, the equal response from the two adjacent filters will cause the filter to update the states to reflect the true orientation of the line strokes. In this way, the Kalman filter refines the coarse approximation of the line-stroke orientations obtained by the Gabor filter.

The results obtained show that paper-based scribbles may be simplified and represented as single line profiles which can subsequently be vectorized. This simplification and vectorization allows the scribbled drawing to be automatically imported into a CAD system. In future, the simplification proposed in this paper may be used in conjunction with a paper-based drawing interface such as [BCFB06] to create virtual 3D models directly from the scribbled drawing.

## References

- [BCF\*05] BARTOLO A., CAMILLERI K. P., FABRI S. G., CASSAR T., BORG J. C.: *Image Binarization using the Extended Kalman Filter*. In *Proceedings of the 2nd International Conference in Informatics in Control, Automation and Robotics* (2005).
- [BCFB06] BARTOLO A., CAMILLERI K. P., FARRUGIA P. J., BORG J. C.: *A New Sketch Based Interface using the Grey-level Co-occurrence Matrix for Perceptual Simplification of Paper Based Scribbles*. In *Eurographics Workshop on Sketch Based Interfaces* (September 2006), Stahovich T., Sousa M. C., Jorge J. A., (Eds.), pp. 91–98.
- [EJ04] ESTRADA F. J., JEPSON A. D.: *Controlling the Search for Convex Groups*. Technical Report CSRG-482, Department of Computer Science, University of Toronto, Canada, 2004.
- [FBCG06] FARRUGIA P. J., BORG J. C., CAMILLERI K. P., GRAHAM G.: *A Sketching Alphabet for Paper-Based Collaborative Design*. *NordDesign 2006 Conference* (2006).
- [GPK02] GRIGORESCU S. E., PETKOV N., KRUIZINGA P.: *Comparison of Texture Features Based on Gabor Filters*. *IEEE Transactions on Image Processing* 11, 10 (October 2002), 1160 – 1167.
- [HT06] HILAIRE X., TOMBRE K.: *Robust and Accurate Vectorization of Line Drawings*. *IEEE Transactions on Pattern Analysis and Machine Interpretation* 28, 6 (2006), 890–904.
- [Hub95] HUBEL D.: *Eye, Brain and Vision*. W. H. Freeman, 1995.
- [KQW06] KU D. C., QIN S.-F., WRIGHT D. K.: *Interpretation of Overtracing Freehand Sketching for Geometric Shapes*. In *Proceedings of the 14th International Conference on Computer Graphics, Visualization and Computer Vision* (January 2006), UNION Agency - Science Press, pp. 263–270.
- [KS06] KARA L. B., SHIMADA K.: *Sketch Based Design of 3D Geometry*. In *Eurographics Workshop on Sketch Based Interfaces* (September 2006), Stahovich T., Sousa M. C., Jorge J. A., (Eds.), pp. 59–68.
- [LD99] LIU W., DORI D.: *Sparse Pixel Vectorisation: An Algorithm and Its Performance Evaluation*. *IEEE Trans-*

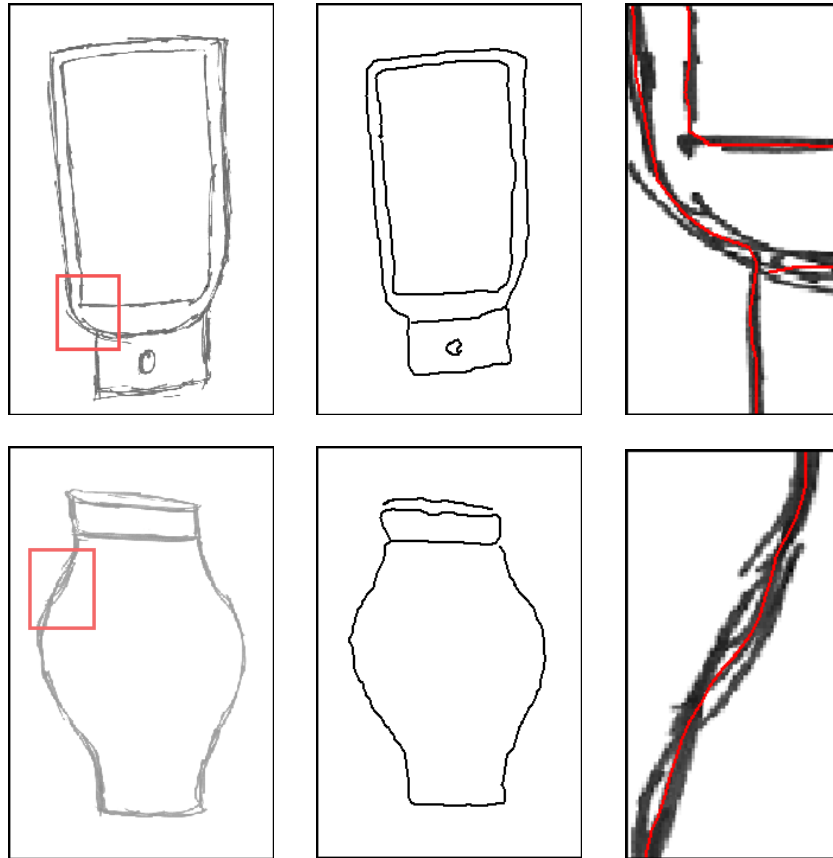


**Figure 10:** The result obtained after using a centre-off filter bank to inhibit the Gabor energy response at the inter-line gaps. Figures (a) to (d) give the original images, whilst Figures (e) to (h) give the Gabor filter results. Figures (i) to (l) give the results obtained by the Kalman filter tracker while Figures (m) and (n) give show the traced trajectory superimposed on the original image for the details highlighted by the red boxes in Figures (a) and (d) respectively

*actions of Pattern Analysis and Machine Intelligence* 21, 3 (1999), 202–215.

[May79] MAYBECK P. S.: *Stochastic Models, Estimation and Control*, vol. 1. Academic Press Inc. (London) Ltd., 1979.

[NM04] NOTOWIDIGDO M., MILLER R. C.: Off-Line Sketch Interpretation. In *AAAI Fall Symposium on Sketch Understanding* (2004), pp. 120–126.

[Sau03] SAUND E.: Finding Perceptually Closed Paths in Sketches and Drawings. *IEEE Transactions on Pattern Analysis and Machine Intelligence* 25, 9 (April 2003), 475–491.

[SD04] SEZGIN T. M., DAVIS R.: Handling Overtraced Strokes in Hand-Drawn Sketches. *Making Pen-Based Interaction Intelligent and Natural* (2004), 1–2.

[SL97] SHPITALNI M., LIPSON H.: Classification of Sketch Strokes and Corner Detection using Conic Sec-

tions and Adaptive Clustering. *Journal of Mechanical Design* 119 (1997), 131–135.

[SSC\*02] SONG J., SU F., CHEN J., TAI C., CAI S.: An Object-Oriented Progressive-Simplification-Based Vectorization System for Engineering Drawings: Model, Algorithm, and Performance. *IEEE Transactions of Pattern Analysis and Machine Intelligence* 24, 8 (2002).